International Journal of Progressive Sciences and Technologies (IJPSAT)
ISSN: 2509-0119.

https://ijpsat.org/

Vol. 57 No. 2 June 2026, pp. 424-434

Schiff Base Ligands As Potential Inhibitors Of Mycobacterium Tuberculosis*: DFT, ADMET Profiling, And Molecular Docking Studies*

Omobola Ajibike Odedokun[2], Kayode Taiwo Ishola[3*] Adebomi Ayodeji Ikotun[1], Chijioke John Ajaelu[1] , Adesoji Adelani Olarenwaju[1], Titilope Adewumi Ajayi[2]

[1]Industrial Chemistry Program, Bowen University, Iwo, Osun State, Nigeria.

[2]Department of Chemistry, Federal College of Education (Special), Oyo, Oyo State, Nigeria

[3]Department of Pure & Applied Chemistry, Ladoke Akintola University of Technology, Ogbomosho, Oyo State, Nigeria.

*Corresponding author: Kayode Taiwo Ishola, ktishola@lautech.edu.ng

Abstract: This study deals with the computational design and assessment antibacterial activities of two Schiff base ligands, specifically L1, identified as (E)-3-((4-aminobenzyl)imino)-1-benzylindolin-2-one, and L2, identified as (Z)-3-((4-aminophenyl)imino)-1-benzylindolin-2-one, with the objective of developing potential therapeutic agents against drug-resistant strains of *Mycobacterium tuberculosis*. Global reactivity parameters, including HOMO/LUMO energies, energy gap, hardness, softness, electronegativity, and electrophilicity of the compounds were ascertained through Density Functional Theory (DFT) computations executed with the ORCA 6.1.1 software package. The SwissADME and ProTox 3.0 platforms were utilized for ADMET profiling to evaluate physicochemical, pharmacokinetic, and toxicological characteristics of the compounds. Molecular docking simulations were conducted against the M. tuberculosis target protein in Dockey. Both ligands were found to adhere to Lipinski's rule of five, suggesting favorable oral bioavailability, and exhibited binding affinities of −9.04 kcal/mol for L1 and −8.82 kcal/mol for L2, thereby exceeding that of the established drug isoniazid (−6.57 kcal/mol). These results indicate that while L1 and L2 serve as promising foundational structures for the development of anti-TB therapeutics, subsequent structural refinement and measures to mitigate toxicity are imperative prior to progression to preclinical stages.

Keywords: ADMET, Docking, Ligand, Tuberculosis, Toxicity

Introduction

Tuberculosis (TB) is an infectious disease caused by bacteria called *Mycobacterium tuberculosis*. The bacteria usually cause an infection in the lungs, but it can affect other parts of the body, such as the kidney, spine, brain, and lymph nodes. If not treated properly, tuberculosis can be fatal. Tuberculosis is spread from person to person through the release of droplets from the lungs or airways of an infected person (Canadian Centre for Occupational Health and Safety (CCOHS), 2025). Tuberculosis (TB) has long been recognized as one of the most ancient and persistent infectious diseases afflicting humanity. Mycobacterium tuberculosis's etiological agent has haunted human populations for millennia, shaping societies and influencing historical events. Despite significant strides in medical science and public health, TB remains a formidable global health challenge, affecting millions of individuals worldwide each year (Alemu.et al., 2021; Davidson et al., 2024). Tuberculosis (TB) is a major public health issue

International Journal of Progressive Sciences and Technologies (IJPSAT)
ISSN: 2509-0119.

https://ijpsat.org/
Vol. 57 No. 2 June 2026, pp. 424-434

around the world, particularly as drug-resistant forms proliferate and routine treatments become less effective. A key concern is Multi-Drug-Resistant Tuberculosis (MDR-TB), which is resistant to at least two of the most potent first-line anti-TB medications, isoniazid (Fig 1c) and rifampin. This renders typical treatment strategies mainly ineffective (CCOHS, 2025. As a result, there is a significant scientific and clinical need to investigate novel chemical entities with strong anti-mycobacterial properties, favourable pharmacological profiles, and the ability to interact effectively with essential biological targets in resistant M. tuberculosis strains.

Many Schiff bases as ligands have received a lot of attention because of their therapeutic properties, and they have been used in various medical fields (Abad Al-Ameer and Shaalan, 2025).

Figure 1 shows two Schiff bases designed from isatins. The goal of this research is to close this gap by designing and computationally assessing new compounds as potential drug-resistant tuberculosis treatments.

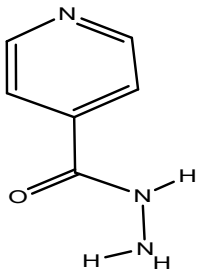

isonicotinohydrazide

Fig 1: Chemical structures of

Methodology

The ORCA software package, the atomistica GUI for ORCA 6.1.1 (Armaković & Armaković, 2023), and the Avogadro molecular visualisation tool were used to perform Density Functional Theory (DFT) calculations to assess the molecular characteristics of the ligands. The ORCA6.1.1 programs (https://www.faccts.de/orca-6-1-1) was used for all computations. PBE0 is the functional used in this study, and it is applied without any symmetry constraints. For non-metallic elements, def2-SVP (Roy et al., 2008) was employed. Additionally included was Grimme's D3 dispersion corrections (Mews et al., 2020; Haseloer et al., 2021). The following global reactivity descriptors were computed using information from the molecular orbital compositions and energy levels: Energy gap (ΔE = Egap = ELUMO −EHOMO), absolute electronegativities (χ = −EHOMO +ELUMO/2), absolute hardness(η = ELUMO − EHOMO/2),chemical potentials (μ = −w), global softness (S = 1/2η), and global electrophilicity (ω = π2/2η) (Sharfalddin et al., 2021; Alomari et al., 2022).

Preparation of the ligands

The ligands were drawn with Chemdraw and Avogdro. The ligands and standard medication were evaluated against a protein called *Mycobacterium tuberculosis* (PDB ID: 1ENZ, resolution 2.70Å). The standard drug's 3D SDF conformer was retrieved from the PubChem Database (https://pubchem.ncbi.nlm.nih.gov).

Preparation of Target Protein and active site analysis

Figure 1 shows the 2.70Å crystal *Mycobacterium tuberculosis* (PDB ID: 1ENZ) from the protein data bank (https://doi.org/10.2210/pdb1ENZ/pdb). All water molecules, heteroatoms, and undesirable complexes were eliminated from the downloaded proteins' crystal structures to prevent unwanted molecular interactions and contaminants using Discovery studio Software v.2020). The prankweb was used to determine the binding pockets and amino acid residues in the active sites of the protein.

International Journal of Progressive Sciences and Technologies (IJPSAT)
ISSN: 2509-0119.

https://ijpsat.org/
Vol. 57 No. 2 June 2026, pp. 424-434

In silico Studies for ADME, drug-likeness, and toxicity prediction

In silico analyses were performed to predict ADME, drug-likeness, and toxicological predictions. The SwissADME web-based tool was used to predict the physicochemical and ADME properties the compounds (Daina *et al*., 2017). Toxicological assessments were carried out utilising the ProTox 3.0 web server (Banerjee *et al*., 2024).

Molecular docking

The ability of the ligands to bind to protein was probed by molecular docking calculations. The target protein was retrieved as crystal coordinates from the protein database. Molecular docking was conducted for compounds and the standard drug using Dockey (Lianming *et al*., 2023). Dockey software utilizes the AutoDockvina docking engine. For the purpose of ensuring comparability, identical receptor structures, grid parameters, and docking configurations were employed. A grid box with dimensions (Angstrom units), x = 20, y = 20, z = 20 and center coordinates x= -0.1637, y=9.0944, z=7.0635 were set up around the protein molecule. The optimized 3D structures of compounds were used for the docking calculations. The binding affinity estimates for different positions of the ligands with protein were retrieved after the docking calculations, and the best binding positions (with the highest binding affinity) were selected for viewing and visualization in Discovery Studio to obtain the interactions of the compounds with protein.

Results and Discussion

Physicochemical and ADMET Properties

Tables 1 and 2 show ADMET properties and toxicity studies obtained for the for the two ligands.

Table 1: ADMET Results for the ligand

Category	Parameter	L1	L2
Druglikeness	Lipinski (L)	Y	Y
	Bioavailability (A)	0.55	0.55
	Molecular Weight (W, g/mol)	341.41	327.38
	LogP	3.24	3.24
	LogS	-4.4	-4.44
Absorption	GI Absorption (G)	Y	Y
	BBB Permeability (B)	Y	Y
	TPSA (Å²)	58.69	58.69
	HBD	1	1
	HBA	2	2
	Rotatable Bonds (R)	4	3
Metabolism	CYP1A2 Inhibition	Y	Y
	CYP2C19 Inhibition	Y	Y
	CYP2C9 Inhibition	Y	Y
	CYP2D6 Inhibition	Y	Y
	CYP3A4 Inhibition	Y	Y

L1= (E)-3-((4-aminobenzyl)imino)-1-benzylindolin-2-one, L2=(Z)-3-((4-aminophenyl)imino)-1-benzylindolin-2-one

International Journal of Progressive Sciences and Technologies (IJPSAT)
ISSN: 2509-0119.

https://ijpsat.org/
Vol. 57 No. 2 June 2026, pp. 424-434

Table 2: Toxicity studies for the ligands

Target	Prediction	
	L1	L2
Carcinogenicity	Active	Active
Immunotoxicity	Inactive	Inactive
Mutagenicity	Active	Active
Cytotoxicity	Inactive	Inactive
BBB-barrier	Active	Active
Ecotoxicity	Active	Active
LD50 (mg/kg)	2000	600
Prediction class	IV	IV

To ascertain the physicochemical and ADMET characteristics of the compounds, designated L1 and L2, they underwent evaluation via SwissADME and Pro-Tox II analyses. The computational assessments encompassed parameters such as lipophilicity (LogP), molecular weight (MW), Abbott bioavailability score, blood–brain barrier (BBB) permeability, solubility (LogS), and gastrointestinal (GI) absorption. Comprehensive details regarding the ADME and toxicity profiles are elucidated in Tables 1 and 2, respectively.

The druglikeness was estimated using Lipinski rule of five which include hydrogen bond acceptor (HBA ≤ 10), hydrogen bond donor (HBD ≤ 5), molecular weight (150 ≤ MW ≥ 500), number of rotable bonds (ROBT ≤ 10), lipophilicity (LogP ≤ 10) (Teague et al., 199; Lipinski, et al., 2004, Veszelka et al., 2018; Haruna et al., 2023). Both L1 and L2 demonstrated full adherence to Lipinski's rule, thereby signifying advantageous oral drug-like properties. Specifically, the molecular weights of L1 (341.41 g/mol) and L2 (327.38 g/mol) are within the permissible range. Furthermore, both compounds exhibited an HBA value of 2 and an HBD value of 1. The presence of 4 rotatable bonds in L1 and 3 in L2 further supports their structural suitability for achieving oral bioavailability. The lipophilicity values (LogP = 3.24 for both compounds) also fall within the acceptable limits. Additionally, both compounds displayed a Topological Polar Surface Area (TPSA) of 58.69 Å², which is substantially below the 140 Å² threshold, indicative of robust membrane permeability. The Abbott bioavailability score for both L1 and L2 was determined to be 0.55, suggesting a moderate level of oral bioavailability. Moreover, both compounds exhibited a high degree of gastrointestinal (GI) absorption, implying efficient uptake upon oral administration.

In contrast to typical medications that do not affect the central nervous system (CNS), both L1 and L2 were anticipated to cross the blood-brain barrier (BBB), suggesting potential CNS effects. While this characteristic could be advantageous for treatments targeting the CNS, it also carries a risk of central side effects, contingent on the intended therapeutic aim. The metabolic assessment indicated that L1 and L2 are projected to inhibit key cytochrome P450 enzymes, specifically CYP1A2, CYP2C19, CYP2C9, CYP2D6, and CYP3A4. This widespread inhibitory capability points to a significant probability of drug-drug interactions, which could result in changes to how drugs are metabolized and potential build-up within the body. L1 and L2 exhibited desirable drug-like qualities, good absorption when taken orally, and suitable physical and chemical characteristics. Nevertheless, their ability to cross the BBB and their potent inhibition of CYP enzymes could present difficulties concerning CNS toxicity and metabolic interactions. These results imply that although the compounds show promise, further refinement is necessary to enhance their safety and metabolic profiles for the purpose of drug development.

Computational toxicological evaluations of compounds L1 and L2 reveal a complex pharmacological profile characterized by substantial safety liabilities are shown in table 4. The prediction class (PC) was used to classify the compounds, Class I and II as fatal if consumed, Class III as toxic if consumed, Class IV as harmful if consumed, Class V perhaps harmful if consumed, Class VI as non- toxic if consumed (Banerjee et al., 2024). Both substances are projected to exhibit carcinogenic and mutagenic properties, thereby conferring long-term risks of genetic damage and oncogenesis, although they are not anticipated to induce immunotoxicity

International Journal of Progressive Sciences and Technologies (IJPSAT)
ISSN: 2509-0119.

https://ijpsat.org/
Vol. 57 No. 2 June 2026, pp. 424-434

or direct cellular damage. The predicted capacity of these compounds to traverse the blood-brain barrier implies potential utility in central nervous system therapies, yet simultaneously introduces apprehension regarding neurotoxic effects.

Acute toxicity assessments yielded median lethal dose (LD_{50}) values of 2000 mg/kg for L1 and 600 mg/kg for L2, classifying them within toxicity class IV, which denotes comparatively low acute toxicity, with L2 exhibiting a greater degree of toxicity. Furthermore, concerns regarding their potential environmental impact are underscored by predicted ecotoxicity. Notwithstanding their low acute toxicity and capacity for blood-brain barrier penetration, the projected carcinogenicity and mutagenicity significantly impede the suitability of L1 and L2 as secure therapeutic agents, thereby mandating further structural modifications and toxicity amelioration strategies prior to preclinical progression.

Global Reactivity Descriptors

Optimized structures of the compounds are shown in Fig 2 and table 3 shows molecular reactivity descriptors for the compounds.

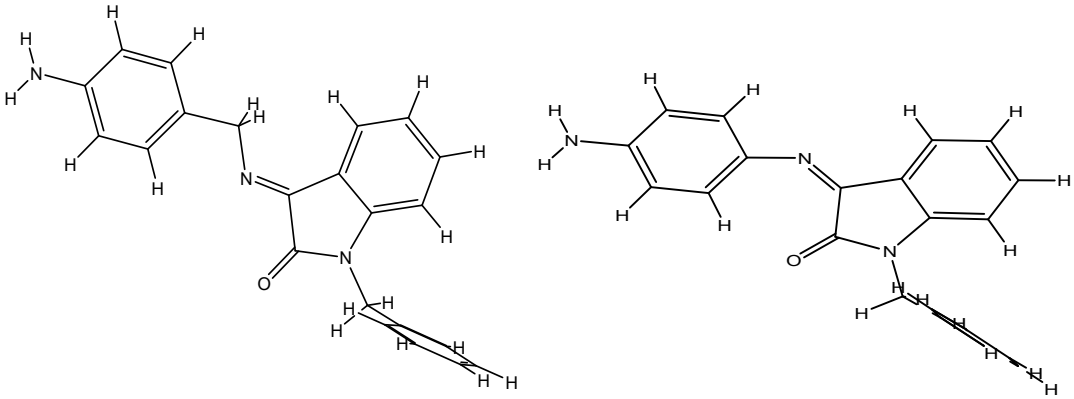

(*E*)-3-((4-aminobenzyl)imino)-1-benzylindolin-2-one (*Z*)-3-((4-aminophenyl)imino)-1-benzylindolin-2-one

Figure 2: Optimized structures of the Schiff base

Table 3: Molecular Reactivity Descriptors for the ligands and the standard drug

Ligand	LUMO (eV)	HOMO (eV)	Eg (eV)	IPo (eV)	EAo (eV)	η (eV)	δ (eV)	χ (eV)	ω (eV)
L1	-2.202	-5.639	3.437	5.639	2.202	1.719	0.582	3.921	4.472
L2	-2.127	-5.276	3.149	5.276	2.127	1.575	0.635	3.702	4.351
ST	-1.848	-7.309	5.461	7.309	1.848	2.731	0.366	4.579	3.839

(Eg= Energy gap; IPo = Ionisation potential; EAo = Electron affinity; η = Hardness; δ = Softness; χ = Electronegativity; ω = Electrophilicity index) L1= (E)-3-((4-aminobenzyl)imino)-1-benzylindolin-2-one, L2=(Z)-3-((4-aminophenyl)imino)-1-benzylindolin-2-one, ST= isoniazid

Molecular descriptors were calculated for the three ligands (L1 and L2) and the standard drug isonicotinohydrazide (ST) using density functional theory (DFT) as shown in Table 3. Figure 2 shows HOMO, LUMO and energy gap diagram. These molecular descriptors were electron affinity (EA), ionization potential (IP), HOMO, LUMO, energy band gap, chemical potential, global electrophilicity index, and chemical hardness. A compound's HOMO is its capacity to give electrons away, whereas its LUMO is its capacity to take them in or take them out. The least reactive and non-polarizable molecule is one with a narrow band gap.

The highest occupied molecular orbitals (HOMO) energies were calculated to be -5.639, -5.276 and -7.848 for L1, L2 and the standard drug, respectively. ST had the higher of HOMO energy than the two ligands. This indicates that the standard drug has the strongest ability to donate electron to the neighboring compounds or atom and to the target protein. LUMO energies were calculated

to be -2.202, -2.127 and -1.848 for L1, L2 and the standard drug, respectively. The LUMO energy indicated that L1 has the strongest ability to accept electron from the target protein, this implies that L1 had high inhibition potential with the target than the drug. The energy gap, Egap, shows a practical guide for the reactivity of the compounds (Sharfalddin et al., 2021). The energy band gaps are 3.437, 3.149 and 5.461 eV. ST had the highest value of energy band gaps indicating higher kinetic stability and low reactivity. L2 had the lowest energy band gaps value facilitating the transfer of electron and high reactivity.

Electron affinities are 2.202, 2.127 and 1.848 eV. L1 had the highest value of EA, indicating that it has the highest capacity to accept electron from other compounds (Asibor et al., 2025). A decrease in chemical hardness corresponds to an increase in reactivity. The values of chemical hardness for the compounds are 1.719, 1.5745 and 2.731 eV. L2 had the lowest value for chemical hardness which implies that it has higher ability to react. Soft molecules (σ) have a small energy gap compared to hard molecules (η), which have a larger energy gap. A soft molecule is more reactive than a hard molecule because a soft molecule has a lower ΔE (LUMO–HOMO). From the table, ST is softer than the two ligands. The (x) is a measure of power of atom(s) to attract the electrons. A high value of electronegativity (χ) suggests strong ability to attract electrons from other compound, which leads to greater interaction to form the complex, decreases according to the following order: ST>L1>L2. Global electrophilicity index are 4.472, 4.351 and 3.839 eV. The molecular descriptors of the Ligands show L1, might have strong interactions with the protein. Figure 2 shows energy diagram for the compounds and the standard drug.

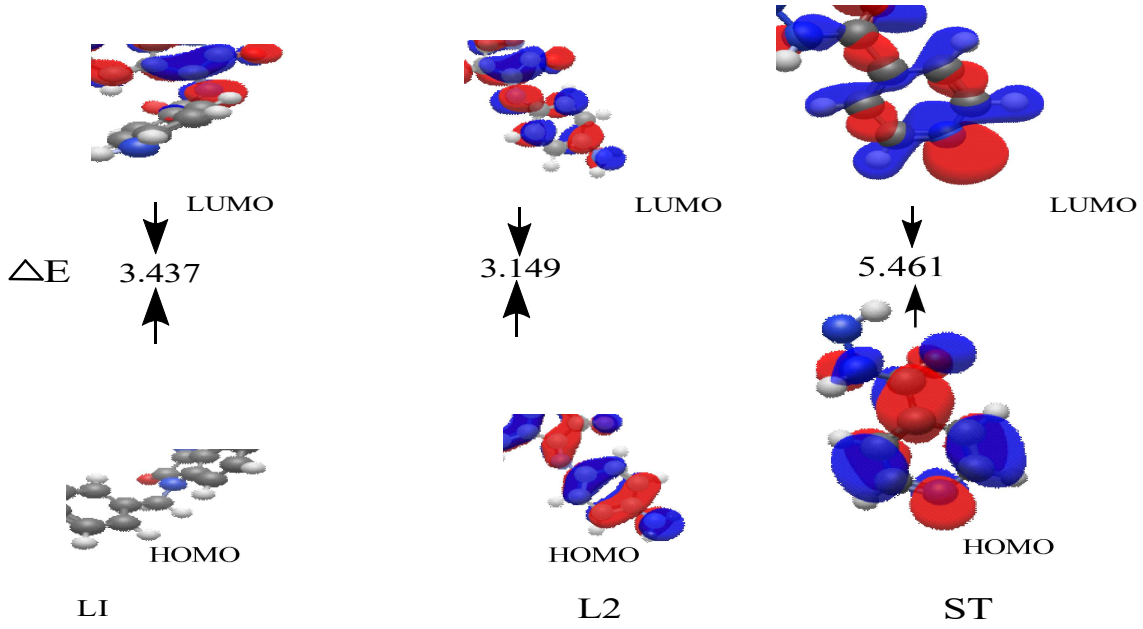

Figure 2: HOMO, LUMO and Energy gap diagram for the ligands and the standard drug.

International Journal of Progressive Sciences and Technologies (IJPSAT)
ISSN: 2509-0119.

https://ijpsat.org/
Vol. 57 No. 2 June 2026, pp. 424-434

Table 4: Interaction Profiles and Binding Affinities of the ligands and the standard drug with

Ligand	Binding Energy	Residue in Contact	Distance	Bond Category	Type
L1	-9.04	GLU18	3.08953	Hydrogen Bond	Conventional Hydrogen Bond
		GLU18	2.61880	Hydrogen Bond	Conventional Hydrogen Bond
		GLU18	3.34367	Hydrogen Bond	Conventional Hydrogen Bond
		GLU8	2.31704	Hydrogen Bond	Conventional Hydrogen Bond
		LYS16	4.28768	Electrostatic	Pi-Cation
		HIS86	4.90163	Electrostatic	Pi-Cation
		HIS86	4.58537	Hydrophobic	Pi-Pi T-shaped
L2	-8.821	GLU18	2.53090	Hydrogen Bond	Conventional Hydrogen Bond
		GLU8	2.07629	Hydrogen Bond	Conventional Hydrogen Bond
		TYR42	2.49777	Hydrogen Bond	Conventional Hydrogen Bond
		ASP57	2.47848	Hydrogen Bond	Conventional Hydrogen Bond
		ASP20	3.42858	Hydrogen Bond	Carbon Hydrogen Bond
		GLU18	4.01442	Electrostatic	Pi-Cation
		HIS21	5.04358	Hydrophobic	Pi-Pi T-shaped
ST	-6.566	GLU8	5.07839	Electrostatic	Attractive Charge
		ASP20	5.01054	Electrostatic	Attractive Charge
		VAL19	2.80524	Hydrogen Bond	Conventional Hydrogen Bond
		HIS21	2.21739	Hydrogen Bond	Conventional Hydrogen Bond
		GLU18	2.08333	Hydrogen Bond	Conventional Hydrogen Bond
		ASP57	3.42295	Hydrogen Bond	Carbon Hydrogen Bond
		LYS16	3.49422	Electrostatic	Pi-Cation

Molecular docking is a reliable procedure which is used to predict binding poses for protein ligand interactions. Thus, this facile study could be exploited to investigate molecular interaction and the most favorable binding site. In addition, the types of interactions based on the distance between the atoms in the amino acid and ligand could also be determined (Gul et al., 2019).

The docking results of the ligands and the standard drug test with the target protein were reported in Table 4. To address the binding interaction of L1.L2 and ST, a 2D interaction of ligand-protein was prepared using BIOVIA Discovery Studio Visualizer (Fig 3). The ligands L1 and L2 had -9.040 and -8.821 kcal/mol, respectively while the standard drugs had -6.566 kcal/mol binding affinity against the target protein, with inhibition constant. L1 and L2 had higher binding affinities and inhibitory potential for tuberculosis cell than the standard drug. As shown in Fig 3, the complex of L1 with the protein exhibited four hydrogen bonding interactions with four amino acid residues (GLU18, GLU18, GLU18 and GLU8), two electrostatic (LYS16 and) and one hydrophobic (HIS86). This result demonstrated that hydrogen bonding and electrostatic interactions could be the key interactions for stabilizing the L1 with the protein in the active site (Latosińska *et al*., 2024).

Furthermore, 2D interaction of L2 with the protein Fig. 3 displayed five hydrogen bonding interactions with five amino acid residues (GLU18, GLU8, TYR42, ASP57 and ASP20). Additionally, electrostatic and hydrophobic interactions were observed with GLU 18 and HIS21, respectively. This finding suggests that the presence of a hydrogen bonding interaction in the ligand with the protein may be a crucial interaction for stabilizing the complex form (Wu, et al., 2020; Mishra et al., 2022; Sugathan et al., 2024). ST interacted with the active site of protein via four conventional Hydrogen bond Val19, Hia21, Glu18 and Asp57, one electrostatic Lys16 (Pi-Cation) and two electrostatic Glu8 and Asp20 (Attractive Charge). The 2D interaction and the surface interactions are shown in the Figure 5.

International Journal of Progressive Sciences and Technologies (IJPSAT)
ISSN: 2509-0119.

https://ijpsat.org/
Vol. 57 No. 2 June 2026, pp. 424-434

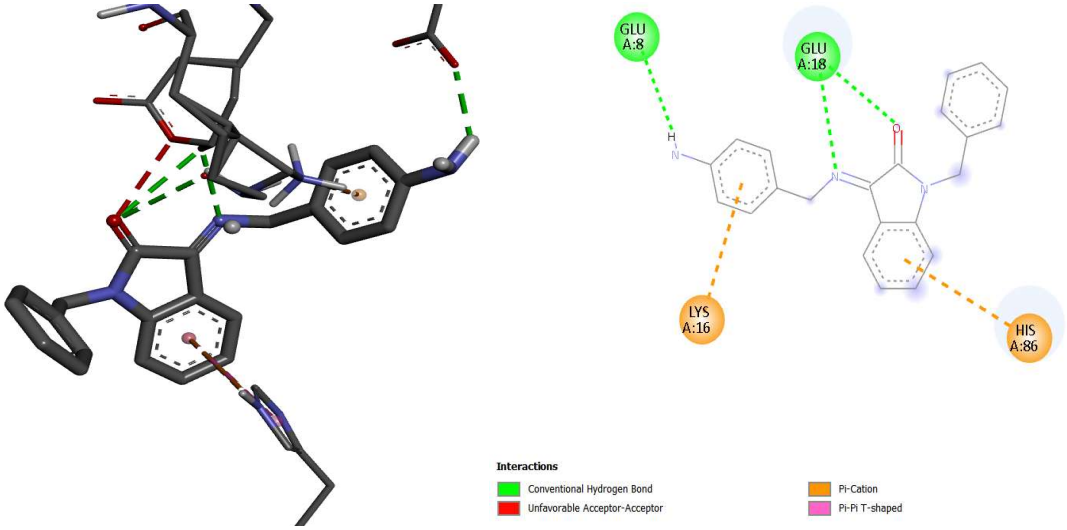

L1

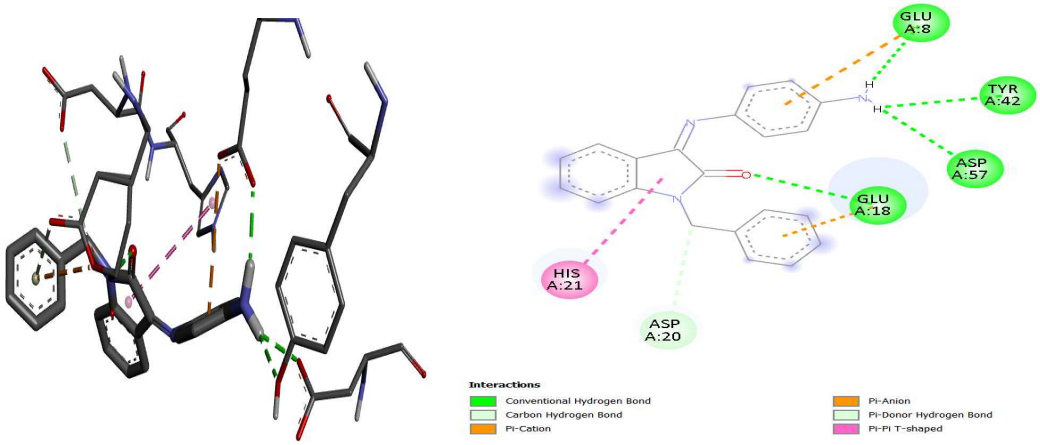

L2

International Journal of Progressive Sciences and Technologies (IJPSAT)
ISSN: 2509-0119.

https://ijpsat.org/
Vol. 57 No. 2 June 2026, pp. 424-434

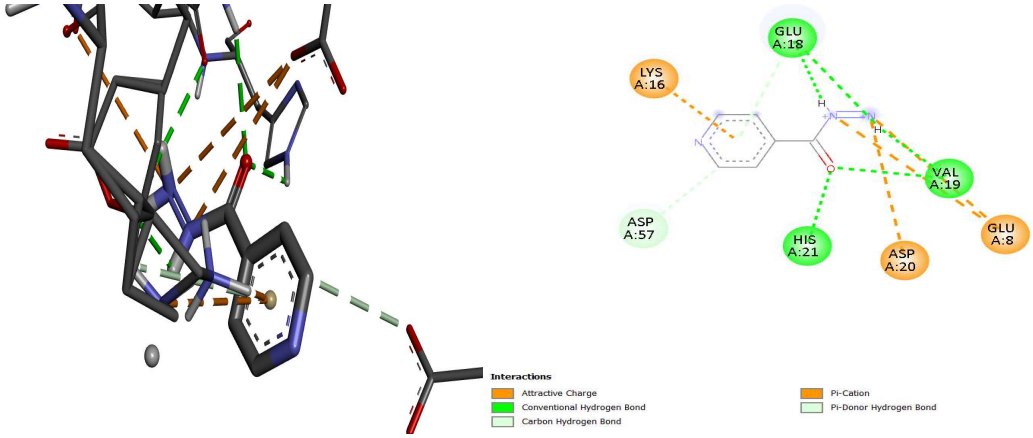

ST

Figure 3: 2D Binding Interactions of the ligands and a standard drug

Conclusion

The two ligands examined exhibit favorable drug-like characteristics and demonstrate superior binding to the tuberculosis target protein compared to the standard drug. Their advantageous physicochemical attributes, efficient oral absorption, and robust molecular interactions suggest their potential as promising lead compounds. However, significant challenges arise from their propensity to induce cancer, alter DNA, penetrate the blood-brain barrier, and inhibit CYP enzymes, all of which necessitate resolution. Further structural refinement and toxicity reduction are essential before these compounds can advance to preclinical development.

References

[1]. Adegbola, P. I., Semire, B., Fadahunsi, O. S. & Adegoke, A. E. (2021). Molecular docking and ADMET studies of Allium cepa, Azadirachta indica and Xylopia aethiopica isolates as potential anti-viral drugs for Covid-19. *Virus Disease* h t t p s : / / d o i . o r g / 1 0 . 1 0 0 7 / s 1 3 3 3 7 - 0 2 1 - 0 0 6 8 2 - 7.

[2]. Alemu A, Bitew ZW, Diriba G, Gumi B. (2021). Occurrence of tuberculosis and diabetes mellitus, and associated risk factors, in Ethiopia: A systematic review and meta- analysis. *IJID*;1:82 91. DOI: 10.1016/j.ijregi.2021.10.004

[3]. Alomari, F.Y.; Sharfalddin, A.A.; Abdellattif, M.H.; Domyati, D.; Basaleh, A.S.; Hussien, M.A.(2022). QSAR Modeling, Molecular Docking and Cytotoxic Evaluation for Novel Oxidovanadium(IV) Complexes as Colon Anticancer Agents. *Molecules*, 27, 649. https://doi.org/ 10.3390/molecules27030649

[4]. Armaković, S. and Armaković, S.J.(2023). Atomistica.Online – Web Application For Generating Input Files For Orca Molecular Modeling Package Made With The Anvil Platform.*Molecular Simulation*, 49 (1), 117 – 123, DOI: 10.1080/08927022.2022.2126865

[5]. Asibor, Y.E, Olatunji, N.O., LATONA1, D. F., Oyebamiji , A.K. and Semire, B. (2025). Swiss Similarity Studies of 5,7-dihydroxy-2-(4-hydroxyphenyl) chromen-4-one: A Promising Role against Sickle cell disease. *International Journal of Health and Pharmaceutical Research* 10(1) www.iiardjournals.orgS

[6]. Banerjee, P., Kemmler E., Dunkel M., Preissner R.(2024). ProTox 3.0: a webserver for the prediction of toxicity of chemicals Nucleic Acids Res (Web server issue).

[7]. Canadian Centre for Occupational Health and Safety (CCOHS), 2025. https://www.ccohs.ca/oshanswers/diseases/tubercul.pdf

[8]. Daina, A., Michielin, O., and Zoete, V. (2017). SwissADME: A free web tool to evaluate pharmacokinetics, drug-likeness and medicinal chemistry friendliness of small molecules, Sci. Rep., 7 (1), 42717.

[9]. Davidson, G., Davidson, D.U., Okoye,O.K., Mensah,L.S., Ukaegbu, E.C., Agbor, D.A., Adegbola,M.O., Eneyo,U.S., Osuluku,B.A., Dinyain,T.O., Okeke,A.A., Okah,M.J., Owulu,A.I., Peterson,J.C., Onyekweli, S.M.,Omoruyi,G.O., Adebiyi,O.S., Atoyebi,F.A.,Omeje,A.C., Ogbueli,O.J.,Odobulu,B.O. and Uche, C.J. (2024). Overview of Tuberculosis: Causes, Symptoms and Risk Factors". *Asian Journal of Research in Infectious Diseases*, 15 (9):8 19. https://doi.org/10.9734/ajrid/2024/v15i9370.

[10]. Dessen, A., Quemard, A., Blanchard, J.S., Jacobs Jr., W.R., Sacchettini, J.C. (1995). Crystal structure and function of the isoniazid target of Mycobacterium tuberculosis.Science **267**: 1638-1641

[11]. Gu, A., Akhter, A. and Siddiq, M. (2019). Molecular Docking and Quantitative Structure Activity Relationship (QSAR) Studies of Some Newly Synthesized Poly (Azomethine) Esters. *International Journal of Polymer Science*. https://doi.org/10.1155/2019/2103891

[12]. Haseloer, A.; Denkler, L.M.; Jordan, R.; Reimer, M.; Olthof, S.; Schmidt, I.; Meerholz, K.; Hörner, G.; Klein, A. (2021). Ni, Pd, and Pt complexes of a tetradentate dianionic thiosemicarbazone-based OˆNˆNˆS ligand. *Dalton Trans.* 50, 4311–4322.

[13]. Haruna, A., Sirajo, I.T., Rumah, M.M. and Albashir, Y. (2023). Synthesis, Characterization, Biological Properties, ADMET and Druglikeness Analysis of Mn (II) complexes with Schiff Bases Derived from Sulphathiazole and 4 diethylaminosalicyaldehyde/Salicyaldehyde, *Int. j. res. appl. sci. biotechnol*., 2(6), 58-68

[14]. Latosińska, M., and Latosińska, J.N. (2024). Favipiravir analogues as inhibitors of SARS-CoV-2 RNA dependent RNA polymerase, combined quantum chemical modeling, quantitative structure property relationship, and molecular docking study. *Molecules*, 29 (2), 441.

[15]. Lianming D., Geng, C., Zeng, Q., Huang, T., Tang, J., Chu, Y. and Zhao, K. (2023). Dockey: A modern integrated tool for large-scale molecular docking and virtual screening. Briefings in *Bioinformatics*, 24(2):bbad047

[16]. Lipinski, C. A. (2004).Lead-and drug-like compounds: The rule-of-five revolution. Drug Discov. Today: Technol. 1(4), 337–343. h t t p s : / / d o i . o r g / 1 0 . 5 7 7 2 / 5 2 6 4 2.

[17]. Mews,N.M.; Reimann, M.; Hörner, G.; Kaupp, M.; Schubert, H.; Berkefeld, A.(2020). A four-parameter system for rationalising the electronic properties of transition metal–radical ligand complexes. *Dalton Trans*. 49, 9735–9742.

[18]. Mishra, A., and Rathore, A.S. (2022). RNA dependent RNA polymerase (RdRp) as a drug target for SARS CoV2*, J. Biomol. Struct. Dyn*., 40 (13), 6039–60351.

[19]. Owonikoko, A.D., Sodamade A., Olatunde, A.M., Odoje, O.F., & Semire, B. (2025). In silico Identification of bioactive compounds from Chasmanthera dependens and Carissa edulis as potential inhibitors of Carbonic anhydrases (CAs) receptors using a target-based drug design approach. *Int. J. Novel Res. Dev*. 9(7), b416-b441

[20]. Roy, L.E.; Hay, P.J.; Martin, R.L. (2008). Revised Basis Sets for the LANL Effective Core Potentials. *J. Chem. Theory Comput*. 4, 1029–1031.

[21]. Sharfalddin, A.A.; Emwas, A.-H.; Jaremko, M.; Hussien, M.A. (2021). Complexation of uranyl (UO2)2+ with bidentate ligands: XRD, spectroscopic, computational, and biological studies. *PLoS ONE*, 16, e0256186.

[22]. Sugathan, K.J., Sreekumar, S., and Kamalan, B.C. (2024). In silico screening and identification of lead molecules from Garcinia gummi-gutta with multitarget activity against SARS-CoV-2. *J. Appl. Pharm. Sci*., 14 (7), 124–132.

[23]. Teague, S.J., Davis, A.M., Leeson, P.D. and Oprea, T. (1999). The Design of Leadlike Combinatorial Libraries, *Angew. Chem. Int. Ed. Engl*., 38, 3743-3748.

[24]. Veszelka, S. et al. (2018). Comparison of a rat primary cell-based blood-brain barrier model with epithelial and brain endothelial cell lines: Gene expression and drug transport. Front. Mol. Neurosci. https://doi.org/10.3389/fnmol.2018.00166.

[25]. Weigend, F. and Ahlrichs, R. (2005). Balanced basis sets of split valence, triple zeta valence and quadruple zeta valence quality for H to Rn: Design and assessment of accuracy. Phys. Chem. Chem. Phys. 7, 3297-3305.

[26]. Wu, Y., Chang, K.Y., Lou, L., Edwards, L.G., Doma, B.K., and Xie, Z.R. (2020). In silico identification of drug candidates against COVID-19. Inf. Med. Unlocked, 21, 100461.

[27]. Yadav, S., Aslam, M., Prajapat, A. et al. (2024) Investigate the binding of pesticides with the TLR4 receptor protein found in mammals and zebrafish using molecular docking and molecular dynamics simulations. Sci Rep 14, 24504. https://doi.org/10.1038/s41598-024-75527-6